

ECE 604, Lecture 33

Fri, April 12, 2019

Contents

1 High Frequency Solutions	2
1.1 Tangent Plane Approximations	2
1.2 Fermat's Principle	3
1.3 Generalized Snell's Law	4
2 Gaussian Beam	5
2.1 Derivation of the Paraxial/Parabolic Wave Equation	5
2.2 Finding a Closed Form Solution	6
2.3 Other solutions	8

1 High Frequency Solutions

1.1 Tangent Plane Approximations

We have learnt that reflection and transmission of waves at a flat surface can be solved in closed form. The important point here is the physics of phase matching. Due to phase matching, we have the law of reflection, transmission and Snell's law.

When a surface is not flat anymore, there is no closed form solution. But when a surface is curved, an approximate solution can be found. This is obtained by using a local tangent-plane approximation when the radius of curvature is much larger than the wavelength. Hence, this is a good approximation when the frequency is high or the wavelength is short. This is similar in spirit that we can approximate a spherical wave by a local plane wave at the spherical wave front when the wavelength is short.

When the wavelength is short, phase matching happens locally, and the law of reflection, transmission, and Snell's law are satisfied approximately as shown in Figure 1. The tangent plane approximation is the basis for the geometrical optics (GO) approximation. In GO, light waves are replaced by light rays. The reflection and transmission of these rays at an interface is estimated with the tangent plane approximation. This is also the basis for lens or ray optics from which lens technology is derived. It is also the basis for ray tracing for high-frequency solutions.

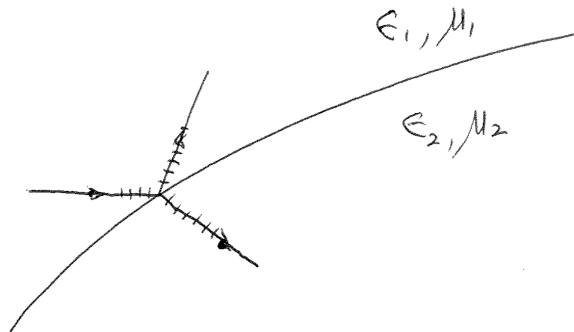


Figure 1:

1.2 Fermat's Principle

Fermat's principle (1600s) says that a light ray follows the path that takes the shortest time between two points.¹ Since time delay is related to the phase delay, and that a light ray can be locally approximated by a plane wave, this can be stated that a plane wave follows the path that has a minimal phase delay. This principle can be used to derive law of reflection, transmission, and refraction for light rays. It can be used as the guiding principle for ray tracing.

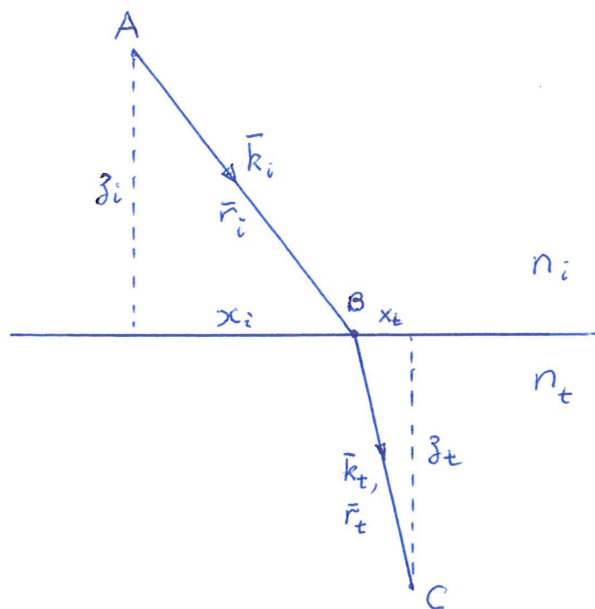


Figure 2:

Given two points A and C in two different half spaces as shown in Figure 2. Then the phase delay between the two points, per Figure 2, can be written as

$$P = \mathbf{k}_i \cdot \mathbf{r}_i + \mathbf{k}_t \cdot \mathbf{r}_t \quad (1.1)$$

As this is the shortest path according to Fermat's principle, another other path will be longer. In other words, if B were to move to another point, a longer path will ensue, or that B is the stationary point of the path length or phase delay. Specializing (1.1) to a 2D picture, then the phase delay as a function of x_i is stationary. In this Figure 2, we have $x_i + x_t = \text{const}$. Therefore, taking

¹This eventually give rise to the principle of least action.

the derivative of (1.1) with respect to x_i , one gets

$$\frac{\partial P}{\partial x_i} = 0 = k_i - k_t \quad (1.2)$$

The above yields the law of refraction that $k_i = k_t$, which is just Snell's law. It can also be obtained by phase matching.

1.3 Generalized Snell's Law

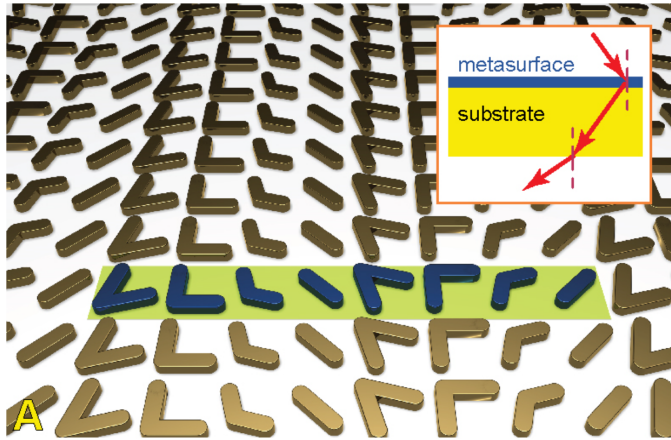


Figure 3: Courtesy of Capasso's group.

Metasurfaces are prevalent these days due to our ability for nano-fabrication and numerical simulation. One of them is shown in Figure 3. Such a metasurface can be thought of as a phase screen, providing additional phase shift for the light as it passes through it. Moreover, the added phase shift can be controlled to be a function of position due to advent in fabrication technology and commercial software for numerical simulation.

To model this phase screen, we can add an additional function $\Phi(x, y)$ to (1.1), namely that

$$P = \mathbf{k}_i \cdot \mathbf{r}_i + \mathbf{k}_t \cdot \mathbf{r}_t - \Phi(x_i, y_i) \quad (1.3)$$

Now applying Fermat's principle that there should be minimal phase delay, and taking the derivative of the above with respect to x_i , one gets

$$\frac{\partial P}{\partial x_i} = k_i - k_t - \frac{\partial \Phi(x_i, y_i)}{\partial x_i} = 0 \quad (1.4)$$

The above yields that the generalized Snell's law (Capasso) that

$$k_i - k_t = \frac{\partial \Phi(x_i, y_i)}{\partial x_i} \quad (1.5)$$

It yields the fact that the transmitted light can be directed to other angles due to the additional phase screen.

2 Gaussian Beam

We have seen previously that in a source free space

$$\nabla^2 \mathbf{A} + \omega^2 \mu \varepsilon \mathbf{A} = 0 \quad (2.1)$$

$$\nabla^2 \Phi + \omega^2 \mu \varepsilon \Phi = 0 \quad (2.2)$$

The above are four scalar equations with the Lorenz gauge

$$\nabla \cdot \mathbf{A} = -j\omega \mu \varepsilon \Phi \quad (2.3)$$

connecting \mathbf{A} and Φ . We can examine the solution of \mathbf{A} such that

$$\mathbf{A}(\mathbf{r}) = \mathbf{A}_0(\mathbf{r})e^{-j\beta z} \quad (2.4)$$

where $\mathbf{A}_0(\mathbf{r})$ is a slowly varying function while $e^{-j\beta z}$ is rapidly varying in the z direction. This is primarily a quasi-plane wave propagating predominantly in the z -direction. We know to be the case in the far field of a source, but let us assume that this form persists less than the far field. Taking the x component of (2.4), we have²

$$A_x(\mathbf{r}) = \Psi(\mathbf{r})e^{-j\beta z} \quad (2.5)$$

where $\Psi(\mathbf{r}) = \Psi(x, y, z)$ is a slowly varying envelope function of x , y , and z .

2.1 Derivation of the Paraxial/Parabolic Wave Equation

Substituting (2.5) into (2.1), and taking the double z derivative first, we arrive at

$$\frac{\partial^2}{\partial z^2} [\Psi(x, y, z)e^{-j\beta z}] = \left[\frac{\partial^2}{\partial z^2} \Psi(x, y, z) - 2j\beta \frac{\partial}{\partial z} \Psi(x, y, z) - \beta^2 \Psi(x, y, z) \right] \quad (2.6)$$

Consequently, after substituting the above into the x component of (2.1), we obtain an equation for $\Psi(\mathbf{r})$, the slowly varying envelope as

$$\frac{\partial^2}{\partial x^2} \Psi + \frac{\partial^2}{\partial y^2} \Psi - 2j\beta \frac{\partial}{\partial z} \Psi + \frac{\partial^2}{\partial z^2} \Psi = 0 \quad (2.7)$$

²Also, the wave becomes a transverse wave in the far field, and keeping the transverse component suffices.

When $\beta \rightarrow \infty$, or in the high frequency limit,

$$\left| 2j\beta \frac{\partial}{\partial z} \Psi \right| \gg \left| \frac{\partial^2}{\partial z^2} \Psi \right| \quad (2.8)$$

In the above, we assume the envelope to be slowly varying and β large, so that $|\beta\Psi| \gg |\partial/\partial z\Psi|$. And then (2.7) can be approximated by

$$\frac{\partial^2 \Psi}{\partial x^2} + \frac{\partial^2 \Psi}{\partial y^2} - 2j\beta \frac{\partial \Psi}{\partial z} \approx 0 \quad (2.9)$$

The above is called the paraxial wave equation. It is also called the parabolic wave equation.³ It implies that the β vector of the wave is approximately parallel to the z axis, and hence, the name.

2.2 Finding a Closed Form Solution

A closed form solution to the paraxial wave equation can be obtained by a simple trick⁴. It is known that

$$A_x(\mathbf{r}) = \frac{e^{-j\beta|\mathbf{r}-\mathbf{r}'|}}{4\pi|\mathbf{r}-\mathbf{r}'|} \quad (2.10)$$

is the solution to

$$\nabla^2 A_x + \beta^2 A_x = 0 \quad (2.11)$$

if $\mathbf{r} \neq \mathbf{r}'$. If we make $\mathbf{r}' = -\hat{z}jb$, a complex number, then (2.10) is always a solution to (2.10) for all \mathbf{r} , because $|\mathbf{r}-\mathbf{r}'| \neq 0$ always. Then

$$\begin{aligned} |\mathbf{r}-\mathbf{r}'| &= \sqrt{x^2 + y^2 + (z+jb)^2} \\ &\approx (z+jb) \left[1 + \frac{x^2 + y^2}{(z+jb)^2} + \dots \right]^{1/2} \\ &\approx (z+jb) + \frac{x^2 + y^2}{2(z+jb)} + \dots, \quad |z+jb| \rightarrow \infty \end{aligned} \quad (2.12)$$

And then

$$A_x(\mathbf{r}) \approx \frac{e^{-j\beta(z+jb)}}{4\pi(z+jb)} e^{-j\beta \frac{x^2+y^2}{2(z+jb)}} \quad (2.13)$$

By comparing the above with (2.5), we can identify

$$\Psi(x, y, z) = A_0 \frac{jb}{z+jb} e^{-j\beta \frac{x^2+y^2}{2(z+jb)}} \quad (2.14)$$

³The paraxial wave equation, the diffusion equation and the Schrodinger equation are all classified as parabolic equations in mathematical parlance.

⁴Introduced by Georges A.Deschamps of UIUC.

By separating the exponential part into the real part and the imaginary part, and writing the prefactor in terms of amplitude and phase, we have

$$\Psi(x, y, z) = \frac{A_0}{\sqrt{1 + z^2/b^2}} e^{j \tan^{-1}(z/b)} e^{-j\beta \frac{x^2+y^2}{2(z^2+b^2)} z} e^{-b\beta \frac{x^2+y^2}{2(z^2+b^2)}} \quad (2.15)$$

The above can be rewritten as

$$\Psi(x, y, z) = \frac{A_0}{\sqrt{1 + z^2/b^2}} e^{-j\beta \frac{x^2+y^2}{2R}} e^{-\frac{x^2+y^2}{w^2}} e^{j\psi} \quad (2.16)$$

where

$$w^2 = \frac{2b}{\beta} \left(1 + \frac{z^2}{b^2}\right), \quad R = \frac{z^2 + b^2}{z}, \quad \psi = \tan^{-1}\left(\frac{z}{b}\right) \quad (2.17)$$

For a fixed z , the parameters w , R , and ψ are constants. Here, w is the beam waist which varies with z , and it is smallest when $z = 0$, or $w = w_0 = \sqrt{\frac{2b}{\beta}}$. And R is the radius of curvature of the constant phase front. This can be appreciated by studying a spherical wave front $e^{-j\beta R}$, and make a paraxial wave approximation, namely, $x^2 + y^2 \ll z^2$ to get

$$\begin{aligned} e^{-j\beta R} &= e^{-j\beta(x^2+y^2+z^2)^{1/2}} = e^{-j\beta z \left(1 + \frac{x^2+y^2}{z^2}\right)^{1/2}} \\ &\approx e^{-j\beta z - j\beta \frac{x^2+y^2}{2z}} \approx e^{-j\beta z - j\beta \frac{x^2+y^2}{2R}} \end{aligned} \quad (2.18)$$

In the last approximation, we assume that $z \approx R$ in the paraxial approximation. The phase ψ changes rapidly with z .

A cross section of the electric field due to a Gaussian beam is shown in Figure 4.

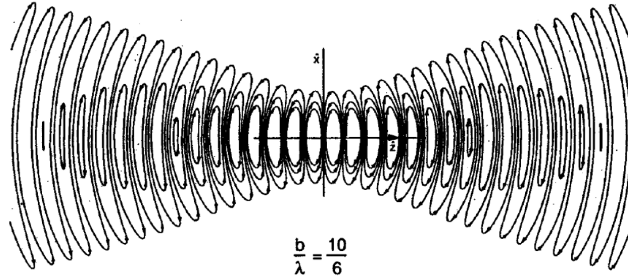


Figure 4: Electric field of a Gaussian beam in the $x - z$ plane frozen in time. The wave moves to the right as time increases; $b/\lambda = 10/6$ (Courtesy of Haus, *Electromagnetic Noise and Quantum Optical Measurements*).

2.3 Other solutions

In general, the paraxial wave equation has solution of the form⁵

$$\Psi_{nm}(x, y, z) = \left(\frac{2}{\pi n! m!} \right)^{1/2} 2^{-N/2} \left(\frac{1}{w} \right) e^{-(x^2+y^2)/w^2} e^{-j \frac{\beta}{2R} (x^2+y^2)} e^{j(m+n+1)\Psi} \quad (2.19)$$

$$\cdot H_n \left(x\sqrt{2}/w \right) H_m \left(y\sqrt{2}/w \right) \quad (2.20)$$

where $H_n(\xi)$ is a Hermite polynomial of order n . The solution can also be express in terms of Laguerre polynomials, namely,

$$\Psi_{nm}(x, y, z) = \left(\frac{2}{\pi n! m!} \right)^{1/2} \min(n, m)! \frac{1}{w} e^{-j \frac{\beta}{2R} \rho^2} e^{-\rho^2/w^2} e^{j(n+m+1)\Psi} e^{jl\phi} \\ (-1)^{\min(n, m)} \left(\frac{\sqrt{2}\rho}{w} \right) L_{\min(n, m)}^{n-m} \left(\frac{2\rho^2}{w^2} \right) \quad (2.21)$$

where $L_n^k(\xi)$ is the associated Laguerre polynomial.

These gaussian beams have rekindled recent excitement in the community because, in addition to carrying spin angular momentum as in a plane wave, they can carry orbital angular momentum due to the complex transverse field distribution of the beams.⁶ They harbor potential for optical communications as well as optical tweezers to manipulate trapped nano-particles. Figure 5 shows some examples of the cross section (xy plane) field plots for some of these beams.

⁵See F. Pampaloni and J. Enderlein.

⁶See D.L. Andrew, Structured Light and Its Applications and articles therein.

Laguerre–Gaussian Beams and Orbital Angular Momentum

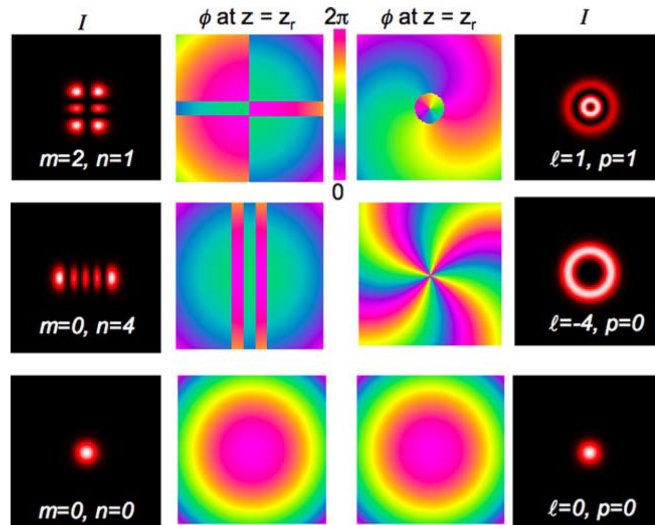


Figure 1.1 Examples of the intensity and phase structures of Hermite–Gaussian modes (*left*) and Laguerre–Gaussian modes (*right*), plotted at a distance from the beam waist equal to the Rayleigh range. See color insert.

Figure 5: Courtesy of L. Allen and M. Padgett's chapter in J.L. Andrew's book on structured light.